Using multi-shaker force control methods in modal analysis

S. Carter[1], D. Rohe[1]
[1] Sandia National Laboratories, Experimental Structural Dynamics,
P.O. Box 5800 – MS0557, Albuquerque, NM, 87185, USA
e-mail: **spcarte@sandia.gov**

Abstract
Shaker excitation is a popular technique in experimental modal analysis because it gives the practitioner a high level of control and repeatability in the excitation. However, the dynamics of the shaker and test article can fundamentally limit the excitation bandwidth when a voltage-mode amplifier is used to power the shaker. Further, multiple shakers can couple to one-another through the test article and correlate the forces during a multiple-input / multiple-output modal test, potentially impacting data quality. This paper will present a study where multi-shaker force control methods are used to remedy these issues through the specification of flat broadband and uncorrelated force spectra. It will discuss the underlying theory to the method as well as the benefits and drawbacks of using force control in modal testing.

1 Introduction

Experimental modal analysis is an extremely popular test technique and is typically conducted using either an impact hammer or electro-dynamic shakers. Impact hammer excitation is a simple method that is widely applicable, but the quality of the resulting frequency response function (FRF) data is highly dependent on practitioner skill. The impacts must be extremely consistent (in location, direction, and amplitude) when using multiple input locations. Otherwise, the FRF matrix will exhibit properties that violate core assumptions in the modal parameter estimation process (such as poor reciprocity, slightly different resonant frequencies for each input location, etc.) [1].

Compared to impact hammers, shakers are more difficult to set-up but provide a more controllable and consistent input. Multiple shakers can be used to simultaneously excite the device under test (DUT), referred to as multiple-input / multiple-output (MIMO) testing. MIMO testing ensures that the FRF data is self-consistent when using multiple input locations, which improves the FRF data quality compared to "one input location at a time" test strategies [2, 3]. A MIMO strategy for impact hammer excitation has also been demonstrated [4], but this technique is not widely used and has not been thoroughly evaluated.

The advantages listed above make shaker excitation an attractive test technique for modal analysis, but there are two significant drawbacks to shaker excitation:

1. The shaker and stinger have vibrating modes in-and-of themselves [5] that can potentially limit the excitation bandwidth.
2. Shakers couple with the structural dynamics of the DUT, potentially causing force drop-outs [6, 7]. Additionally, multiple shakers can couple to one-another through the structural dynamics of the DUT, potentially causing errors in the force measurements and FRF estimation [3]. General wisdom in the modal testing field cautions that the forces in a MIMO modal test should be as uncorrelated as possible [8], meaning that the shakers should be as uncoupled as possible.

A current mode amplifier can be used to mitigate force drop-outs due to the shaker-DUT coupling [7]. However, current-mode amplifiers are specialized equipment that are not always available and may not fully resolve the force drop-out issue [6]. Additionally, a current-mode amplifier will not influence the structural

coupling between multiple shakers. Consequently, an alternative test technique is needed to mitigate the effects of the shaker-DUT coupling.

This paper will describe a technique, that uses multi-shaker force control (MFC) methods to ensure that the excitation forces are uncorrelated and have flat power spectral densities (PSDs) in the desired frequency range. The remainder of this paper is organized as follows:

1. Basic theory to describe the shaker-DUT coupling.
2. The control theory and process for the MFC modal testing technique.
3. An example of using the proposed MFC technique in a simulated beam modal test to illustrate the theory.
4. An example of using the MFC technique in an experimental modal test on an academic structure.
5. Concluding remarks that discuss of the benefits and drawbacks of using MFC modal testing.

2 Basic theory for shaker-DUT coupling

The shaker-DUT coupling can be modeled using frequency based substructuring (FBS) [9, 10]. The FBS theory will be illustrated with the example beam test set-up that is shown in Figure 1, where the beam is being excited at two locations simultaneously with shakers in a MIMO test configuration. The FBS equation to compute the response of the beam due to a voltage supplied to the shakers is shown in (1). The FBS equation in (1) can be broken down into component equations that describe the response on the beam due to the shaker/beam interface force and the shaker/beam interface force due to the supplied excitation voltage [11], as shown in (2) and (3). Note that the shaker/beam interface force is what would be measured as the reference force in a modal test and will simply be referred to as the "force" for the rest of this paper. The notation for all three equations is described in Table 1. Curly brackets, $\{\cdot\}$, indicate a vector quantity in the equations and square brackets, $[\cdot]$, indicate a matrix quantity. It should be noted that all the quantities in (1), (2), and (3) are frequency dependent, but this notation has been excluded from the equations for brevity.

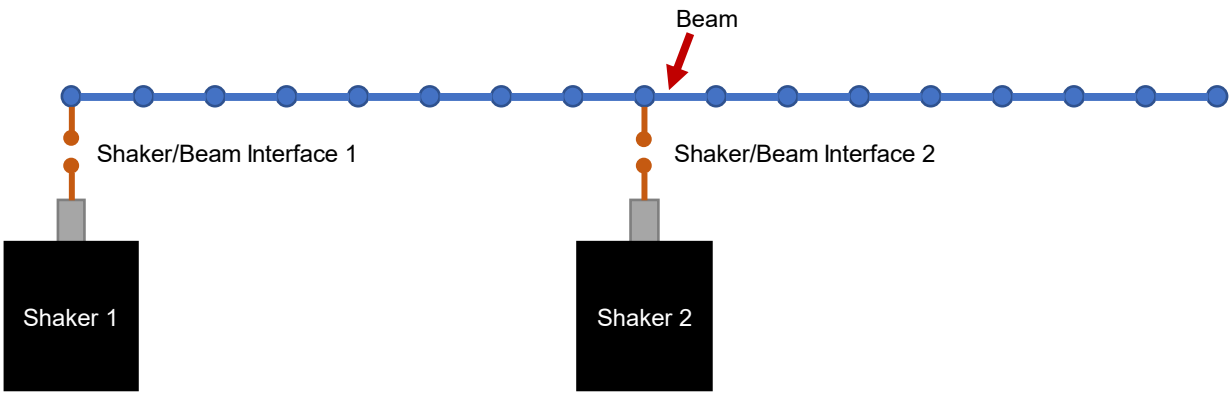

Figure 1: Example shaker set-up on a beam

The influence of the coupling between the beam and shakers on the force is obvious in (3) which shows that the force is dependent on the modal behavior of both the beam and shakers. The dependence on modal behavior means that the force spectra will contain resonances and anti-resonances that correspond to the modes of the beam and shakers. Further analysis of (3) also highlights some of the reasoning behind the common rules of thumb for shaker selection [1, 3, 8]:

- The practitioner should select excitation locations on the structure that are dynamically independent from one another. This will reduce the off-diagonal terms in $\left[H_{ii}^{beam}\right]$ in (3), which will reduce the coupling between the shaker forces. Note that the off-diagonal terms in the shaker FRF matrices are zero since the shakers are uncoupled from each another.
- The shaker armature and stinger should be as light as possible (compared to the DUT). This will increase the amplitude of the FRFs in $\left[H_{ii}^{shaker}\right]$ in (3), which will make the shaker FRFs more significant to the force compared to the DUT (beam) FRFs.

$$\{x_r^{beam,shaker}\} = [H_{ri}^{beam}]([H_{ii}^{beam}] + [H_{ii}^{shaker}])^{-1}[H_{is}^{shaker}]\{v_s\} \quad (1)$$

$$\{x_r^{beam,shaker}\} = [H_{ri}^{beam}]\{f_i^{beam,shaker}\} \quad (2)$$

$$\{f_i^{beam,shaker}\} = ([H_{ii}^{beam}] + [H_{ii}^{shaker}])^{-1}[H_{is}^{shaker}]\{v_s\} \quad (3)$$

Table 1: Notation for the FBS equation

Quantity	Description
$\{x_r^{beam,shaker}\}$	The response on the beam (denoted by the subscript r). The "beam,shaker" superscript implies that this is the response of the coupled beam-shaker system.
$[H_{ri}^{beam}]$	The FRF matrix describing the response/force relationship between the response locations (denoted by the subscript r) and forces at the shaker/beam interface locations (denoted by the subscript i). The "beam" superscript implies that these FRFs are from the beam when it is detached from the shakers.
$[H_{ii}^{beam}]$ & $[H_{ii}^{shaker}]$	The FRF matrices describing the response/force relationship at the shaker/beam interface locations (denoted by the subscript i). The beam superscript implies that FRFs are from the beam when it is detached from the shakers and the "shaker" superscript implies that the FRFs are from shakers detached from the beam.
$[H_{is}^{shaker}]$	The FRF matrix describing the response/voltage relationship between the shaker/beam interface locations (denoted by the subscript i) and the voltage input to the shaker or amplifier, depending on preference (denoted by the subscript s). The "shaker" superscript implies these FRFs are from the shakers detached from the beam.
$\{v_s\}$	The voltage input to the shaker or amplifier, depending on preference (denoted by the subscript s). This quantity does not have a superscript because it is independent of both the beam and shakers.
$\{f_i^{beam,shaker}\}$	The beam-shaker interface force (denoted by the subscript i). The "beam,shaker" superscript implies that this is a force in the coupled beam-shaker system.

3 MFC theory and technique

MFC is identical to the standard MIMO vibration control strategy [12, 13], except MFC uses forces as the target quantity instead of responses. This control strategy is based on the FRF equation of motion with power spectra, as shown in (4), where $[G_{ff}]$ is the target force cross-power spectral density (CPSD) matrix, $[H]$ is the control FRF matrix (the force/voltage FRFs between the forces and voltage input to the amplifier), $[G_{vv}]$ is the drive voltage CPSD matrix (the voltage sent to the amplifier), and $[\cdot]^*$ indicates the conjugate transpose of a given matrix. Note that the CPSD format makes it easy to specify the amplitude, phase, and correlation between the forces, which is why it is preferred over linear spectra and time traces.

$$[G_{ff}] = [H][G_{vv}][H]^* \quad (4)$$

The drive voltages are estimated with the inverse problem that is shown in (5), where $[\cdot]^\dagger$ indicates the pseudo-inverse of the given matrix.

$$[G_{vv}] = [H]^\dagger[G_{ff}][H]^{\dagger^*} \quad (5)$$

The MFC technique is extremely flexible, and the practitioner can specify a wide variety of force CPSD matrices, as long as the specified forces are within the controllable space of the test set-up. This flexibility is a significant benefit for MIMO vibration testing but can also present a significant challenge since the practitioner needs to generate specifications at all the target degrees of freedom (DOFs). Fortunately, MFC

modal testing does not require complicated specifications since uncorrelated forces with flat broadband PSDs should be sufficient for most tests. These forces can be easily specified with an identity matrix that has been scaled to the desired force RMS levels. As a result, the practitioner only needs to determine an appropriate force RMS level for the test, rather than specifying a potentially complicated set of power spectra.

The process for MFC modal testing (excluding the test activities that are common to every modal test) is:

1. Generate the target force CPSD matrix, $[G_{ff}]$, using the scaled identity approach that was described above.
2. Measure the (force/voltage) control FRFs, this is referred to as the system identification (ID) phase of the test. Note that the system ID data (if measured at all the force and response DOFs) is equivalent to traditional modal test data.
3. Perform quality checks on the system ID data and decide whether to proceed with the test, depending on the results of the quality checks. Typical quality checks for the system ID data are:
    a. Perform a signal to noise ratio (SNR) check for the force DOF measurements to ensure that the forces can be measured with reasonable accuracy.
    b. Perform a coherence check between the drive voltage DOFs and force DOFs to ensure that there are not external sources (or non-linearities) acting on the system that could degrade the controllability of the test.
    c. Check the conditioning of the control FRF matrix (condition number, number of independent singular values, etc.) to ensure that the inverse problem in (5) well posed.
4. Compute the drive voltage CPSD matrix, $[G_{vv}]$ with the inverse problem in (5).
5. Perform quality checks on the estimated drive voltage CPSD matrix and decide whether to proceed with the test depending on the results of the quality checks. Typical quality checks on the drive voltage CPSD matrix are:
    a. Reconstruct the forces from the estimated drives using (4) and compare them to the target forces to ensure that the control is reasonably accurate.
    b. Check that the drive voltage peak and RMS levels are reasonable for the shakers and amplifiers that are being used.
6. Synthesize the drive voltage time signals from the CPSD matrix [14] and play them through the shaker system. The voltage time signals could either be random, periodic random, or burst random [15], depending on the desired excitation scheme.

The test process and control strategy outlined above have been formulated through the collective expertise and experience of multiple staff members at Sandia National Labs over several MIMO vibration tests. It seems reasonable to assume that standard practices from a MIMO vibration test will be applicable to an MFC modal test, but specialized processes may be required, based on the slightly different test goals. It should also be noted that MIMO vibration testing is a large and growing field, so different and better test practices may be available.

4 Simulated beam modal test with and without force control

An MFC and uncontrolled (i.e., traditional) MIMO modal test of the beam set-up that was shown in Figure 1 was simulated to evaluate the MFC technique. The test-up was virtually assembled using the FBS scheme that was described in Section 2, using the beam and shakers as separate substructures. The FRFs for the beam were generated from a finite element (FE) model that was generated with two dimensional (shear and moment) Euler-Bernoulli beam elements in SDynPy [16], using the properties that are listed in Table 2. The damping ratio for each mode in the model was set to 0.05%.

The shakers were substructured to the beam at the nodes that are shown in Figure 1, where each dot represents a node in the FE model. The shaker FRFs for the substructuring scheme were experimentally measured on a Modal Shop K2007E01 shaker with integrated amplifier. Note that the shakers were attached to the beam in the shear direction only (i.e., no moment excitation). Also, it was assumed that the stinger was infinitely rigid with no buckling (i.e., a flexible element was not modeled for the stinger).

Table 2: Geometric and material properties for the beam model

Property	Quantity
Elastic Modulus	68.947573 GPa
Poisson's Ratio	0.33
Density	2698.8 kg/m^2
Beam Cross-section Width	0.03 m
Beam Cross-section Height	0.03 m
Beam Length	1 m
Number of Elements	16

4.1 Process for simulating the beam modal test

The beam modal test was simulated using the following process with the test parameters that are listed in Table 3. Note that the forces in the MFC modal test were specified to have the same RMS as the forces as the uncontrolled modal test.

1. 100 realizations (one realization per measurement average) of normally distributed burst random excitation were generated in the time domain to represent the voltage input for each shaker in the simulation. The time domain signals were converted to the linear spectra via a discrete Fourier transform so the responses could be computed via FRFs. The shaker drive voltages were computed using the following techniques for the different test types:
    a. **Uncontrolled Test:** The voltages were generated with the `burst_random` function in SDynPy (which uses `numpy.random.randn` [17]).
    b. **MFC Test:** The process described in Section 3 was used to generate the drive voltages.
2. The FBS formulation in (2) and (3) was used to compute the forces and response for every realization of the burst random excitation, resulting in 100 realizations of unaveraged linear force and response spectra for each shaker.
3. Noise was added to both the force and response linear spectra using the following process:
    a. 100 realizations (one realization per measurement average) of white noise were generated using `numpy.random.randn`. The noise time signal was scaled to have the same peak amplitude as the bin size in a 24 bit analog to digital converter (ADC) with a +/- 20 V range (which was chosen to accentuate noise errors). A separate noise signal was generated for each response and force DOF in the simulation.
    b. The noise time signals were converted to linear spectra via a discrete Fourier transform.
    c. The responses and forces were converted from engineering to voltage units based on a 10 mV/g and 10 mV/N sensitivity.
    d. The noise spectra from step b were added to the linear voltage spectra from step c to compute the "noised" response and force spectra in electrical units.
    e. The noised response and force voltage spectra from step d were converted back to physical units using the sensitivities from step c.
4. The autopower and cross-power spectra were computed and averaged from the noised response and force linear spectra.
5. The FRFs and coherence were computed from the averaged autopower and crosspower spectra. The H1 FRF estimator [18] was used in this work, because it is extremely common in modal testing.

Table 3: Test parameters for the simulated modal test

Property	Quantity
Excitation Type	Burst Random
Burst Pre-trigger	5%
Burst On Percentage	60%
Window Type	Uniform
Sampling Frequency	8,192 Hz
Frequency Resolution	1 Hz
Number of Averages	100
Averaging Type	Linear

4.2 Simulated modal test results

The complex mode indicator function [19] (CMIF) for the simulated modal test with uncontrolled forces, compared to the truth CMIF (computed from the FRFs of the FE model) is shown in Figure 2. The CMIF shows that there are significant errors in the peaks of the FRFs from the simulated test with uncontrolled forces. This error is also seen in the multiple coherence for the simulated test with uncontrolled forces, as shown in Figure 3 for a sample response DOF, where there are significant drops in the coherence at the resonance frequencies (note that all the response DOFs had similar coherence).

As explained above, the error in the FRF estimation is due to the shaker-beam coupling (which also results in shaker-shaker coupling). The shaker-beam coupling is obvious when reviewing the force PSDs, as shown in Figure 4, where there are significant drop-offs at the natural frequencies of the beam. These force drop-offs cause low amplitude responses, resulting in measurements with a low SNR that cause errors in the FRF estimation. The shaker-shaker coupling is also obvious when reviewing the correlation between the force DOFs, as seen in the high coherence levels between the force DOFs in Figure 5. Note that the high correlation between forces can also contribute to errors in the FRF estimation, but experience has shown that the measurement noise is the primary source of error.

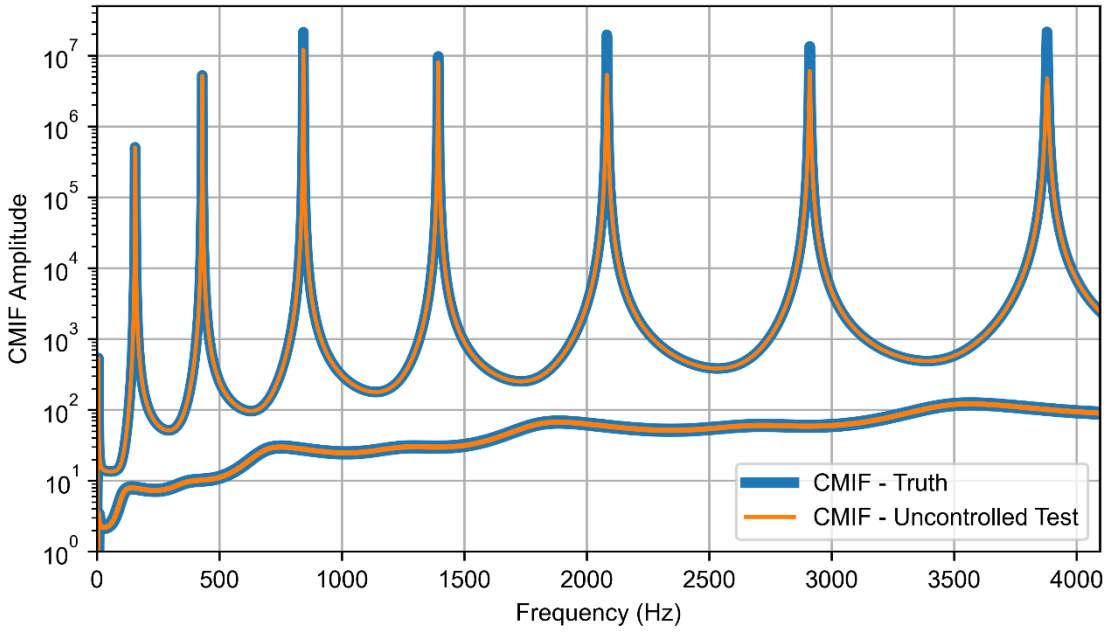

Figure 2: CMIF from the simulated uncontrolled modal test compared to the truth CMIF

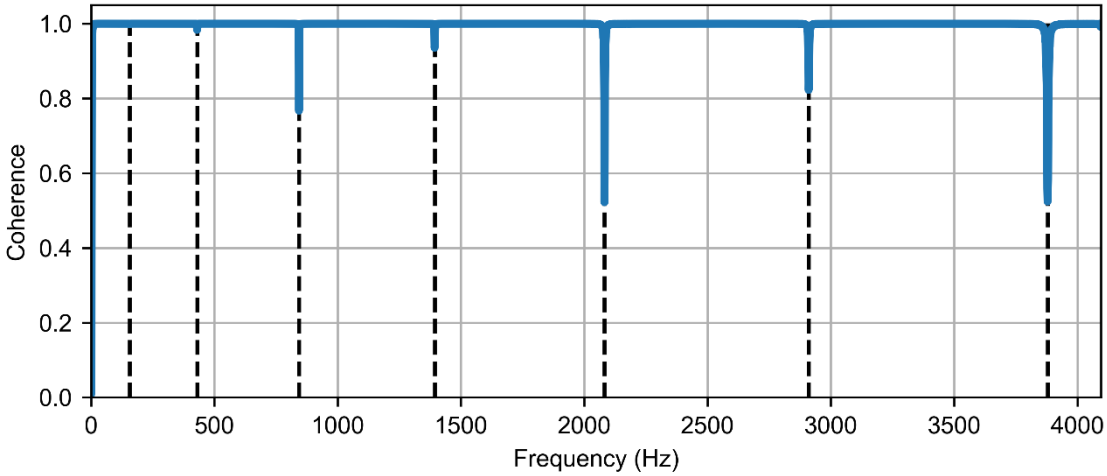

Figure 3: Multiple coherence for the sheer response at the right tip of the beam from the simulated uncontrolled modal test, the vertical dashed lines are the natural frequencies of the beam

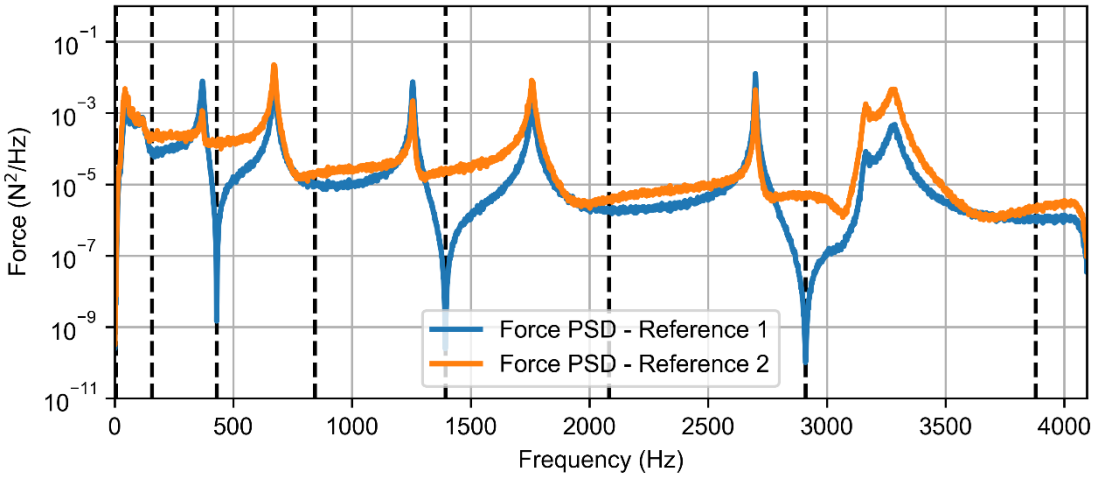

Figure 4: Force PSDs from the simulated uncontrolled modal test, the vertical dashed lines are the natural frequencies of the beam

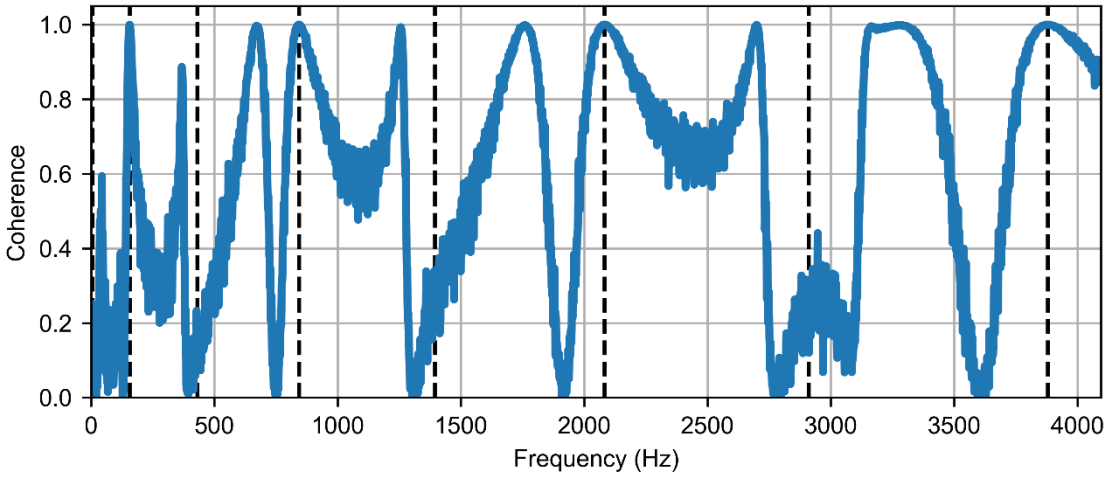

Figure 5: Coherence between the force DOFs for the simulated uncontrolled modal test, the vertical dashed lines are the natural frequencies of the beam

The results for the simulated MFC modal test are significantly better than the results for the uncontrolled modal test. There is line-on-line similarity between the truth and MFC test CMIFs, as shown in Figure 6. Also, the coherence for the MFC test is one over the entire frequency range, as shown in Figure 7 for a sample response DOF. A significant drawback of the MFC modal test is that it requires much greater drive voltages than the uncontrolled modal test. The increases in drive voltages for the beam test are shown in Figure 8 where the drive voltage RMS level is ~90-140 times greater for the MFC modal test. Note that standard pseudoinverse control is notoriously inefficient, and more efficient control techniques are available [20] but were deemed unnecessary for this simulated test.

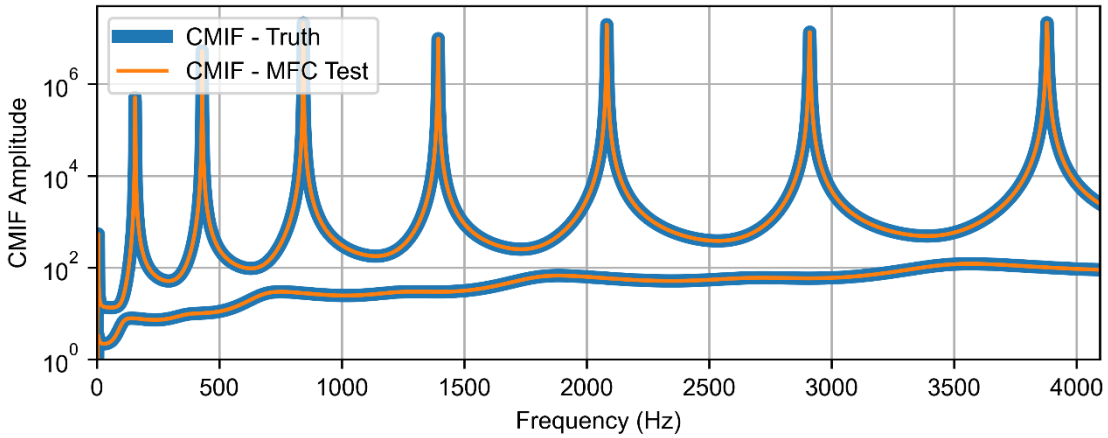

Figure 6: CMIF from the simulated MFC modal test compared to the truth CMIF

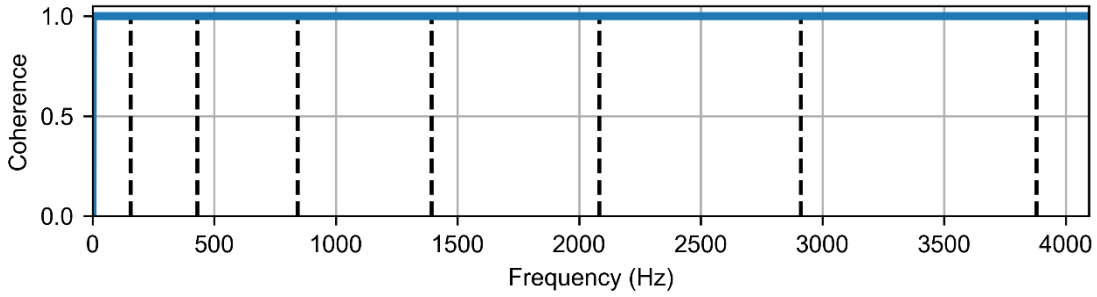

Figure 7: Multiple coherence for the shear response at the right tip of the beam from the simulated MFC modal test, the vertical dashed lines are the natural frequencies of the beam

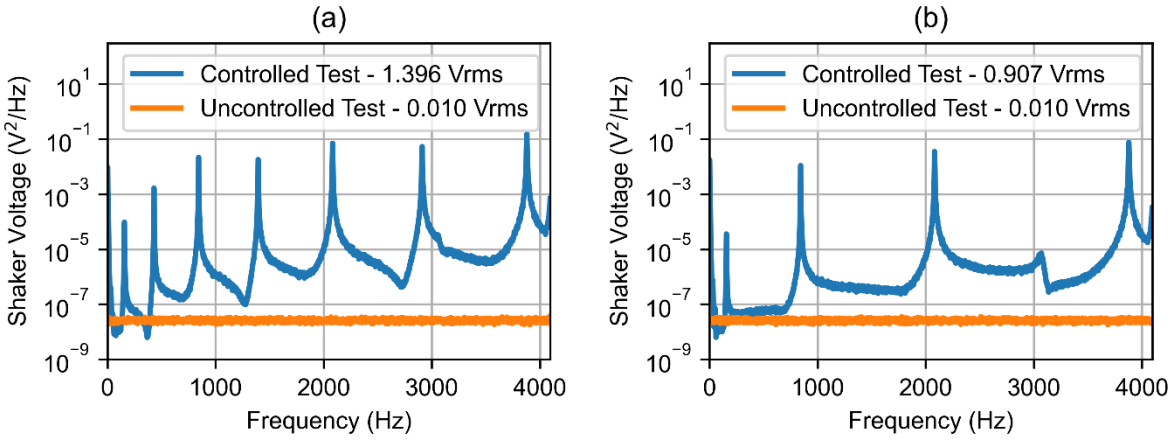

Figure 8: Shaker drive voltages for the simulated MFC modal test compared to the simulated modal test with uncontrolled forces: (a) shaker 1, (b) shaker 2

5 Example test results on an academic structure

An MFC modal test was performed on the “cylinder-plate-beam” (CPB) academic structure to illustrate the benefits the MFC modal test method in an actual test. The CPB is composed of a cylinder with plates bolted to either end; a beam that extends inside of the cylinder is bolted to one of the plates. A cutaway view of the CPB is shown in Figure 9.

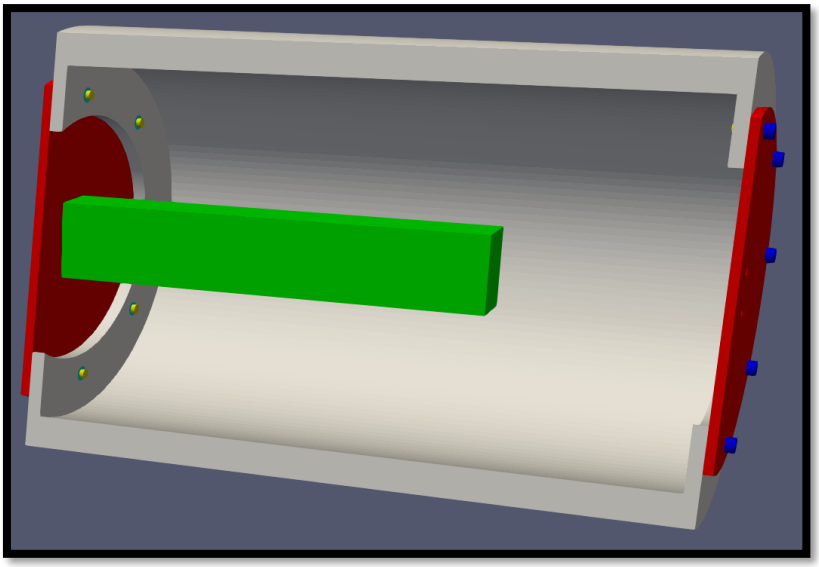

Figure 9: Cutaway view of the CPB structure

5.1 CPB test set-up

The CPB test set-up is shown in Figure 10 and was developed using optimization techniques. Effective independence was used to the determine accelerometer locations [21], with a budget of 28 triaxial accelerometers. Three Modal Shop model 2100E11 100lb shakers were used to excite the CPB. The shaker locations were selected with the “differential evolution” optimization function in SciPy [22], where the cost function was the dB error in a synthesized MIMO vibration test. Note that the shakers are label one, two, and three in ascending order from the lowest to highest shaker in Figure 10.

The test was performed using the “MIMO Random Vibration” environment in the Rattlesnake Vibration Controller software [23]. Both the MFC and uncontrolled modal tests were performed using random excitation with the data acquisition and processing parameters that are shown in Table 4. Random excitation was used in this test (instead of burst random) because it is the only excitation type in the random vibration control module of rattlesnake.

Table 4: Test parameters for the CPB test

Property	Quantity
Excitation Type	Random
Window Type	Hann
Sampling Frequency	8,192 Hz
Frequency Resolution	2 Hz
Number of Averages	100
Averaging Type	Linear

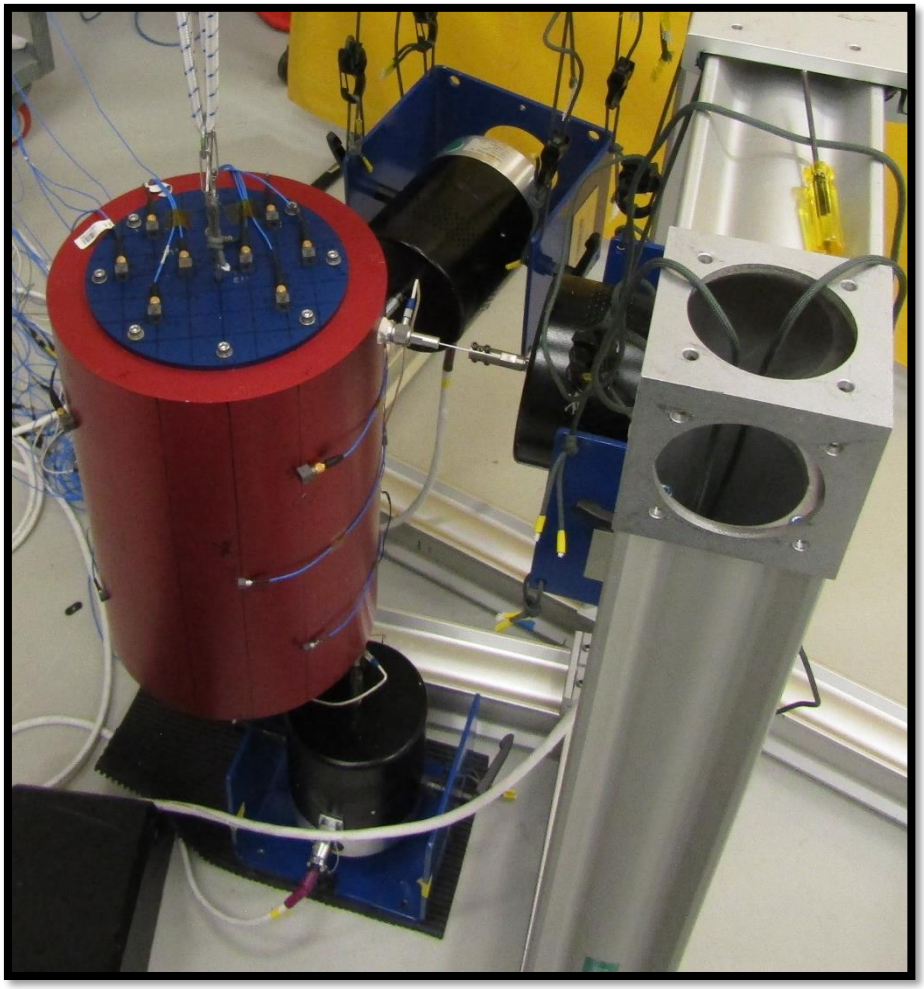

Figure 10: CPB test set-up

The MFC modal test used the process that was described in Section 3, where the force levels were scaled to have the same RMS levels as the uncontrolled modal test, as listed in Table 5. The test used the "pseudoinverse control" control law that is prepackaged with the Rattlesnake software [24] with the "update transfer function" option turned on. Also note that the test was performed with a low frequency cut-off at 30 Hz to avoid the low frequency control issues that are common in MIMO vibration testing.

Table 5: Force specification RMS levels for the CPB test

Shaker	Force RMS Level (N)
1	0.69
2	0.57
3	0.58

5.2 CPB test results

The force PSDs and singular values of the force CPSD matrices for the MFC and uncontrolled CPB modal tests are shown in Figure 11 and Figure 12. The force PSDs for the uncontrolled test show a significant resonance at ~600-750 Hz, after which there is significant roll-off in the force amplitudes. This resonance (and roll-off) is due to the stinger and is unavoidable unless the stinger is eliminated, based on previous experience with the shaker system. The MFC technique mitigates the stinger effects since the force PSDs

are flat to ~3,600 Hz. It is assumed that the force roll-off at higher frequencies in the MFC test is due to the anti-aliasing filters in the data acquisition system and could be eliminated by changing the sampling rate or specification frequency range. The force singular values show that all the forces were uncorrelated from each other in both the MFC and uncontrolled CPB modal tests. Consequently, the main difference in the excitation for the MFC and uncontrolled CPB modal tests is that the MFC test has significantly more excitation energy at high frequencies (>750 Hz).

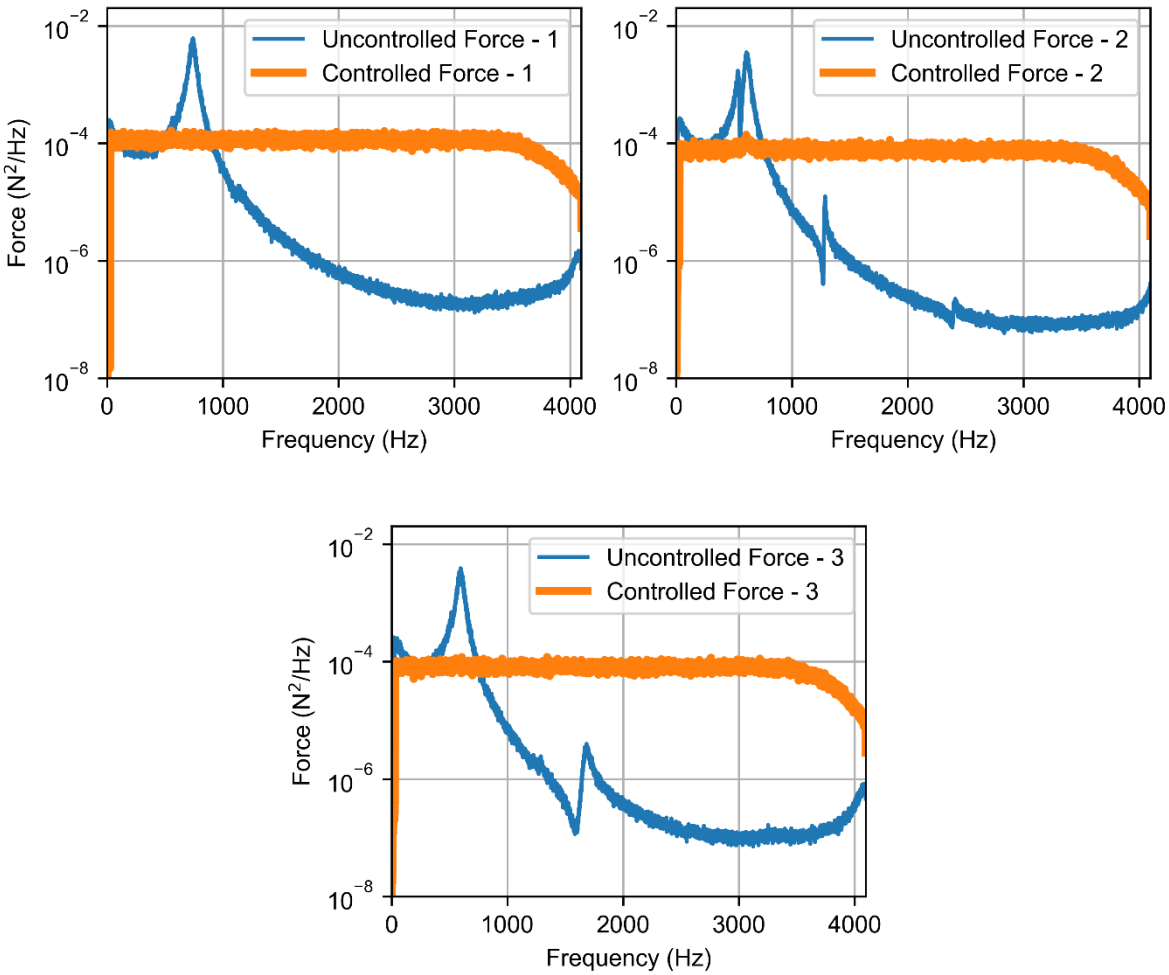

Figure 11: Forces from uncontrolled and MFC modal test on the CPB

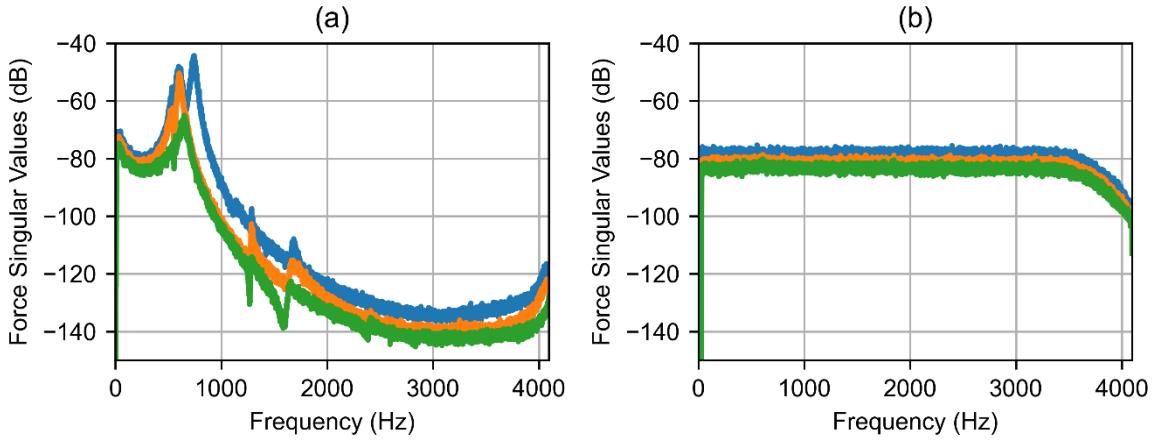

Figure 12: Singular values of the force CPSD matrix for the CPB modal test: (a) uncontrolled, (b) MFC

The FRFs and coherence for the CPB modal tests are shown in Figure 13 and Figure 14 for a sample response DOF that is representative of all the response DOFs in the tests. The most obvious difference in the FRFs and coherence is that there is much lower noise in the high frequency data for the MFC test compared to the uncontrolled test. As mentioned above, the MFC test has much higher excitation energy than the uncontrolled test at high frequencies. The higher excitation energy results in higher response amplitudes, which increases the signal to noise ratio and improves the data quality.

Further inspection of the FRFs revealed that there were some moderate differences in the shape of the FRFs at high frequencies for the MFC and uncontrolled modal tests. The exact reason for the changes in the FRFs is unknown and extensive testing was done to ensure that these changes were not caused by errors in the test technique. It was assumed that the changes in the FRFs were due to non-linear response, since the CPB was designed to have a non-linear response. This finding seems to highlight the importance of selecting an appropriate excitation strategy to properly excite and understand the modes of interest. The MFC technique could be of great use in this situation since it allows for significant control over the excitation.

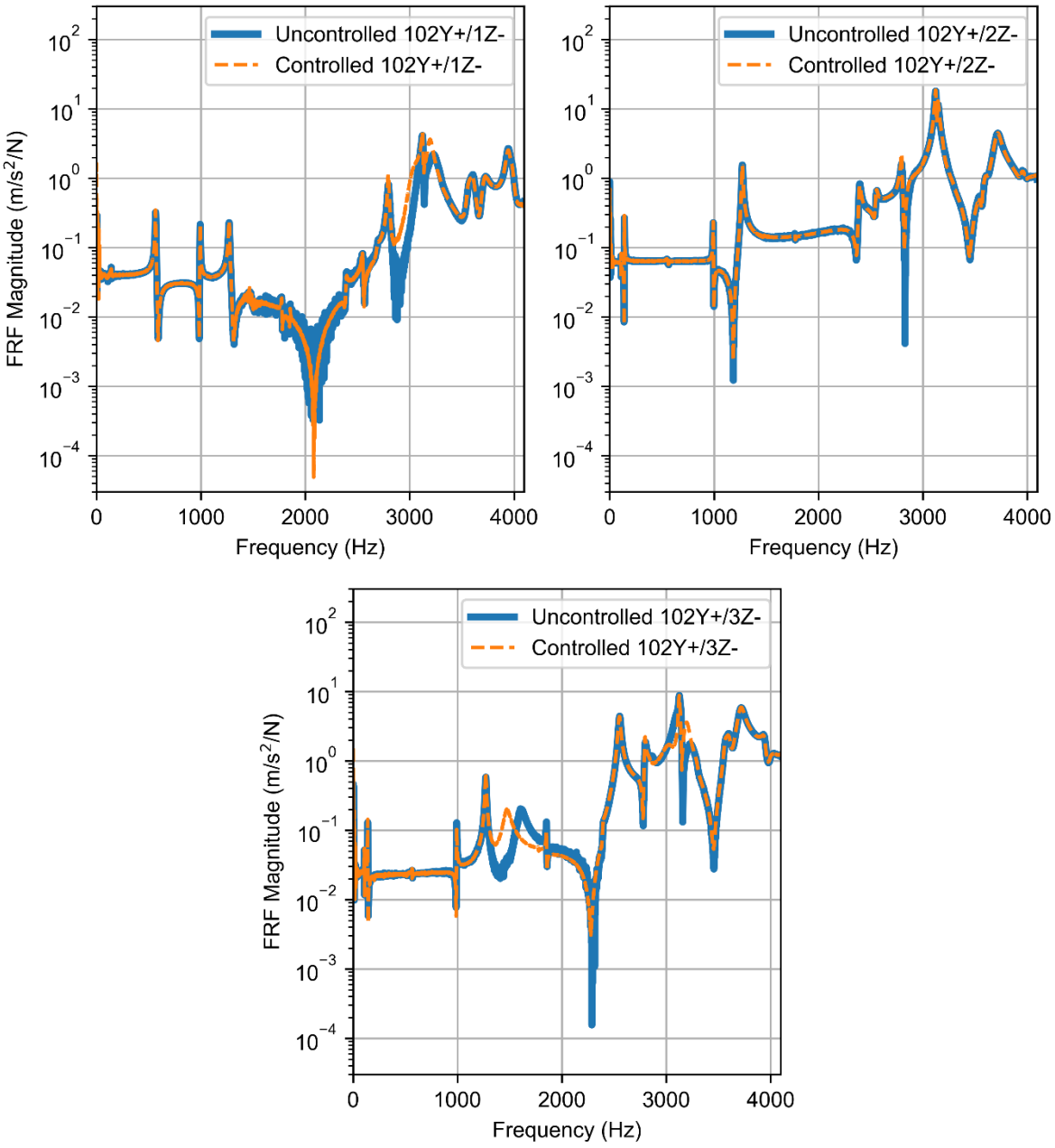

Figure 13: FRF comparison between the uncontrolled and MFC modal tests on the CPB at a sample response DOF

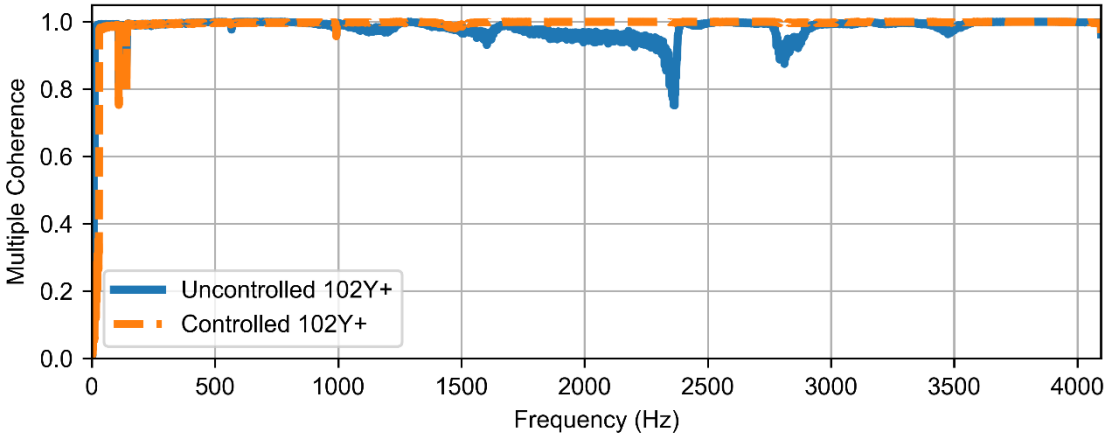

Figure 14: Multiple coherence comparison between the controlled and MFC modal tests on the CPB at a sample response DOF

The MFC technique in the CPB modal test was much less efficient than the uncontrolled technique, with the MFC technique requiring drive voltages with ~15-27x higher amplitudes than the uncontrolled test. The difference in the drive voltage amplitudes was much less significant in the CPB test compared to the simulated beam test and it is assumed that this is because the CPB has much higher damping than the beam (reducing the amplitude of the resonances). The drive voltages were well within the capability of the shaker system, so the higher drive voltages did not influence the test operation. It should also be noted that the non-linear response required that the control FRFs be updated throughout the test, which required the use of MIMO vibration control software. The control FRF updating was required because the FRFs significantly changed from one excitation level to another, as discussed above. Consequently, a test that didn't use control FRF updating would result in erroneous peaks in the forces (since the control is accounting for resonances and anti-resonances that have changed in frequency).

6 Conclusions and suggestions for future work

The theory and results presented in this work imply that the MFC modal test technique is generally superior to the traditional, uncontrolled modal test technique with shakers. Both the numerical and experimental examples showed significant improvements in data quality with the MFC technique compared to the uncontrolled technique. The MFC technique mitigates the force drop-outs, resonances, and roll-off that can be seen when using the uncontrolled technique, which is the primary reason why the MFC technique produces higher quality data than the uncontrolled technique. Further, the MFC technique ensures that the excitation forces in a MIMO set-up are uncorrelated from each other, which is typically desirable in modal testing.

There are two main disadvantages to the MFC modal test technique. The primary disadvantage is that the MIMO control technique requires specialized test software. However, open-source software (such as Rattlesnake) and several commercial packages (such as Siemens Simcenter Test.Lab) have been developed to perform MIMO vibration tests and could be used for MFC modal testing. The second disadvantage is that the MFC technique can require significantly greater drive voltages than the uncontrolled technique, depending on the DUT modes, test set-up, and test parameters. However, the authors experience has shown that MFC drive voltages are within the capabilities of typical modal shakers and amplifiers.

Future work should focus on evaluating more elegant control techniques, such as Tikhonov regularization, to reduce the required drive voltages. Initial work has shown that regularization can dramatically reduce the drive voltages while achieving flat force PSDs, but the forces become correlated to one-another. Other future work should investigate methods for determining the appropriate force levels and spectra shapes in a modal test since the MFC technique makes it possible to specify a wide variety of force spectra, which was historically not an available option.

Acknowledgements

The author would like to thank Ryan Schultz for his advice and inspiration throughout this project.

This article has been authored by an employee of National Technology & Engineering Solutions of Sandia, LLC under Contract No. DE-NA0003525 with the U.S. Department of Energy (DOE). The employee owns all right, title and interest in and to the article and is solely responsible for its contents. The United States Government retains and the publisher, by accepting the article for publication, acknowledges that the United States Government retains a non-exclusive, paid-up, irrevocable, world-wide license to publish or reproduce the published form of this article or allow others to do so, for United States Government purposes. The DOE will provide public access to these results of federally sponsored research in accordance with the DOE Public Access Plan ***https://www.energy.gov/downloads/doe-public-access-plan*** .

Sandia National Laboratories is a multimission laboratory managed and operated by National Technology & Engineering Solutions of Sandia, LLC, a wholly owned subsidiary of Honeywell International Inc., for the U.S. Department of Energy's National Nuclear Security Administration under contract DE-NA0003525.

References

[1] E. L. Peterson, "Modal excitation: Good data not bad data," in *Proceedings-SPIE The International Society for Optical Engineering*, 1993, pp. 1161-1161.

[2] M. A. Peres, C. Kallmeyer, M. C. Witter, R. Carneiro, F. D. Marques, and L. P. R. de Oliveira. (2015) Advantages of Multiple-Input Multiple-Output testing. *Sound and Vibration*. 8-12.

[3] P. Avitabile, "4.5 Multiple-input, Multiple-output Measurement," in *Modal Testing: A Practitioners Guide*. Hoboken, NJ: John Wiley & Sons Ltd., 2018.

[4] P. Avitabile, "A Mixed Impact Shaker MIMO Test Technique (MIS-MIMO)," in *Proceedings of IMAC-XL, the 40th International Modal Analysis Conference*, Orlando, 2022.

[5] G. F. Lang and D. Snyder. (2001) Understanding the physics of electrodynamic shaker performance. *Sound and Vibration*. 24-33.

[6] P. Varoto and L. de Oliveira, "On the Force Drop Off Phenomenon in Shaker Testing in Experimental Modal Analysis," *Shock and Vibration*, vol. 9, pp. 165-175, 01/01 2002, doi: 10.1155/2002/675674.

[7] E. L. Peterson, T. A. Mouch, and W. M. Rusen. (1990) Modal Excitation: Force Drop-off at Resonance. *Sound and Vibration*.

[8] D. J. Ewins, "3.13.4 Multi-point Random (MPR) Testing," in *Modal Testing: Theory, Practice, and Application*, 2 ed. Bladock, Hertfordshire, England: Research Studies Press Ltd., 2000.

[9] R. Schultz, "Vibration Test Design with Integrated Shaker Electro-Mechanical Models," in *Dynamic Substructures, Volume 4, Proceedings of the 38th IMAC, A Conference and Exposition on Structural Dynamics*, 2020, pp. 63-72.

[10] P. Fickenwirth, J. Schultze, D. Harvey, and M. Todd, "Shaker Capability Estimation Through Experimental Dynamic Substructuring," in *Dynamic Environments Testing*, vol. 7, 2023, pp. 151-162.

[11] M. V. van der Seijs, D. de Klerk, and D. J. Rixen, "General framework for transfer path analysis: History, theory and classification of techniques," *Mechanical Systems and Signal Processing*, vol. 68-69, pp. 217-244, 2016/02/01/ 2016, doi: **https://doi.org/10.1016/j.ymssp.2015.08.004**.

[12] *MIL-STD-810H: Method 527.2 Multi-Exciter Test*, U.S. Department of Defense, 2019.

[13] P. Daborn, "Smarter dynamic testing of critical structures," PhD dissertation, Aerospace Department, University of Bristol, 2014.

[14] R. A. Schultz and G. D. Nelson, "Input Signal Synthesis for Open-Loop Multiple-Input/Multiple-Output Testing," in *Sensors and Instrumentation, Aircraft/Aerospace, Energy Harvesting & Dynamic Environments Testing, Volume 7*, Cham, C. Walber, P. Walter, and S. Seidlitz, Eds., 2020// 2020: Springer International Publishing, pp. 245-257.

[15] W. Heylen, S. Lammens, and P. Sas, *Modal Analysis Theory and Testing*. Katholieke Universiteit Leuven, Faculty of Engineering, Department of Mechanical Engineering, Division of Production Engineering, Machine Design and Automation, 1998.

[16] D. Rohe, "SDynPy: A Structural Dynamics Python Library," in *Proceedings of IMAC XLI, the 41st International Modal Analysis Conference*, Austin, 2023.

[17] C. R. Harris *et al.*, "Array programming with NumPy," *Nature*, vol. 585, no. 7825, pp. 357-362, 2020/09/01 2020, doi: 10.1038/s41586-020-2649-2.

[18] R. J. Allemang, R. S. Patwardhan, M. M. Kolluri, and A. W. Phillips, "Frequency response function estimation techniques and the corresponding coherence functions: A review and update," *Mechanical Systems and Signal Processing*, vol. 162, p. 108100, 2022/01/01/ 2022, doi: **https://doi.org/10.1016/j.ymssp.2021.108100**.

[19] C. Y. Shih, Y. G. Tsuei, R. J. Allemang, and D. L. Brown, "Complex mode indication function and its applications to spatial domain parameter estimation," *Mechanical Systems and Signal Processing*, vol. 2, no. 4, pp. 367-377, 1988/10/01/ 1988, doi: **https://doi.org/10.1016/0888-3270(88)90060-X**.

[20] R. Schultz, "A Demonstration of Force Estimation and Regularization Methods for Multi-Shaker Testing," in *Proceedings of IMAC XXXVII, the 37th International Modal Analysis Conference*, Houston, 2020, doi: 10.1007/978-3-030-12676-6_21.

[21] D. C. Kammer and M. L. Tinker, "Optimal placement of triaxial accelerometers for modal vibration tests," *Mechanical Systems and Signal Processing*, vol. 18, no. 1, pp. 29-41, 2004/01/01/ 2004, doi: **https://doi.org/10.1016/S0888-3270(03)00017-7**.

[22] P. Virtanen *et al.*, "SciPy 1.0: fundamental algorithms for scientific computing in Python," *Nature Methods*, vol. 17, no. 3, pp. 261-272, 2020/03/01 2020, doi: 10.1038/s41592-019-0686-2.

[23] D. Rohe and R. Schultz, "Rattlesnake: An open-source multi-axis and combined evironments vibration controller," in *Proceedings of IMAC-XL, the 40th International Modal Analysis Conference*, Orlando, 2022.

[24] D. Rohe, R. Schultz, and N. Hunter, "Rattlesnake User's Manual," Sandia National Laboratories, 2021.